AD_____

Award Number: W81XWH-10-1-0752

TITLE: Engineered PlyCB as a Novel Implant Coating for Osseointegration

PRINCIPAL INVESTIGATOR: Daniel Nelson

CONTRACTING ORGANIZATION: University of Maryland
College Park, MD 20742

REPORT DATE: March 2012

TYPE OF REPORT: Final

PREPARED FOR: U.S. Army Medical Research and Materiel Command
Fort Detrick, Maryland 21702-5012

REPORT DOCUMENTATION PAGE

Form Approved
OMB No. 0704-0188

1. REPORT DATE *(DD-MM-YYYY)*	2. REPORT TYPE	3. DATES COVERED *(From - To)*
01-03-2012	Final	1 SEP 2010 - 29 FEB 2012

4. TITLE AND SUBTITLE
Engineered PlyCB as a Novel Implant Coating for Osseointegration

5a. CONTRACT NUMBER

5b. GRANT NUMBER
W81XWH-10-1-0752

5c. PROGRAM ELEMENT NUMBER

6. AUTHOR(S)
Daniel Nelson

E-Mail: nelsond@umd.edu

5d. PROJECT NUMBER

5e. TASK NUMBER

5f. WORK UNIT NUMBER

7. PERFORMING ORGANIZATION NAME(S) AND ADDRESS(ES)
University of Maryland
College Park, MD 20742

8. PERFORMING ORGANIZATION REPORT NUMBER

9. SPONSORING / MONITORING AGENCY NAME(S) AND ADDRESS(ES)
U.S. Army Medical Research and Materiel Command
Fort Detrick, Maryland 21702-5012

10. SPONSOR/MONITOR'S ACRONYM(S)

11. SPONSOR/MONITOR'S REPORT NUMBER(S)

12. DISTRIBUTION / AVAILABILITY STATEMENT
Approved for Public Release; Distribution Unlimited

13. SUPPLEMENTARY NOTES

14. ABSTRACT

During the performance period, we successfully constructed five RGD or cyclic-RGD containing mutants to PlyCB. Four of them were to the N-terminus and one was to the external loop between helicies 1 and 2 of PlyCB. All five mutants were expressed, purified, and analyzed to confirm retention of wild-type properties. These tests included analytical gel filtration/dynamic light scattering (to confirm self assembly of PlyCB into an octameric ring) and thermal denaturation studies by circular dichroism (to confirm proper protein folding and thermalstability properties). We found that addition of RGD or cyclic RGD did not affect any of the wild-type biochemical or biophysical properties when added to the N-terminus of PlyCB. Next, we tested the binding of mutants to hydroxyapatite (HA) under various salt, pH, phosphate, and temperature conditions. Under all conditions, the mutants strongly and completely bound HA. Three N-terminal mutants were chemically crosslinked to a fluorophore for visualization by fluorescent microscopy. We used the labeled constructs to demonstrate specific binding of our PlyCB-RGD mutant to αvβ3 integrins, osteoblasts, and concurrent binding to HA-coated titanium and osteoblasts. Thus, we have successfully engineered the biotic/abiotic orthopedic surface to promote osseointegration.

15. SUBJECT TERMS
RGD, integrin, binding, osteoblast, hydroxyapatite, titanium implant, bioactive coating

16. SECURITY CLASSIFICATION OF:			17. LIMITATION OF ABSTRACT	18. NUMBER OF PAGES	19a. NAME OF RESPONSIBLE PERSON
a. REPORT	b. ABSTRACT	c. THIS PAGE			USAMRMC
U	U	U	UU	15	19b. TELEPHONE NUMBER *(include area code)*

Table of Contents

INTRODUCTION:

Orthopedic implant materials are often not compatible with osteoblasts, bone cells responsible for formation of new bone. The lack of osseointegration is the primary cause of implant failure or shortened lifespan under physiological loads. Coatings such as hydroxyapatite, the mineral component of bone, are often used to promote integration of bone with implant. However, hydroxyapatite coatings do not contain any inherent bioactive properties. Integrins are a family of bioactive proteins that promote adherence of osteoblasts to extracellular matrix proteins. Significantly, the tri-peptide sequence Arg-Gly-Asp, or "RGD", is sufficient to direct binding to several of the predominant integrins including $\alpha_v\beta_3$, which is displayed by osteoblasts (Morra, 2006). Engineering orthopedic surfaces to display proteins or short peptides such as RGD is an ongoing challenge to the biomaterial field (Carson, 2007; Tsiridis, 2007; Axelrad, 2007; Schuler, 2006). Interestingly, PlyCB, a bacteriophage-derived protein, was found to have a particularly high affinity for hydroxyapatite (Nelson, 2006). Based on the crystal structure, we plan to introduce mutants to PlyCB that will display the RGD motif and hopefully retain the natural ability of this protein to bind hydroxyapatite. The biochemical and biophysical properties of PlyCB when bound to hydroxyapatite will be investigated by several methods. Finally, a sandwich of titanium implant, hydroxyapaptite coating, and PlyCB-RGD mutants will be made and binding to cultured osteoblasts will be determined by fluorescent binding assays. Future proposals will be aimed at *in vivo* implant models to show increased osteoblast formation on PlyCB-RGD treated implants. Additionally, we envision the ability to display other "bone-stimulating factors" on the surface of PlyCB in future proposals.

BODY:

Aim 1. Make PlyCB-RGD mutants.

Task 1. Obtain reagents. (month 1)

All reagents have been obtained. In particular, we ordered several osteoblast cell lines from the American Type Culture Collection and have worked out the optimum conditions for growth, division, maintenance, and storage of these cells that will be used for Aim 3. In addition, we identified a supplier for hydroxyapatite-coated titanium discs that can be used in 24-well tissue culture flasks as well as for microscopy studies to mimic an orthopedic implant.

Task 2. Make RGD mutations to PlyCB (i.e. PlyCB-RGD). (months 2-6)

To make PlyCB bioactive toward recruitment of osteoblasts, we added RGD sequence motifs to several strategic locations through point-directed mutagenesis based on the crystal structure. PlyCB is 72 amino acids, but self-assembles into an octamer. It has an accessible N-terminus as well as a solvent-exposed, external loop between helices 1 and 2 (at amino acid 21) that are suitable for engineering RGD sequence motifs. As such, we introduced the RGD sequence to the N-terminus and in between amino acids 21 and 22 as shown in Fig. 2a and 2e, respectively. In addition, we had concerns about the stability of the N-terminal 8 amino acids of PlyCB. These 8

amino acids do not show electron density in the crystal structure but are predicted to form a beta barrel by *in silico* modeling. If these 8 residues did not possess stable secondary structure, then we feared our addition of RGD to the extreme N-terminus would not be exposed to the solvent front. Therefore, we decided to delete the first 8 amino acids. In this mutant (Fig. 2b), the N-terminal RGD sequence is attached to amino acid number nine. Finally, several publications suggest that integrins bind the RGD motif when it is constrained in a cyclical fashion rather than displayed in a linear peptide. We therefore constructed the "4C" mutant whereby two cysteine residues are added to either side of the RGD motif (i.e. CCRGDCC). The cysteine residues would then interact through disulfide bridges causing the RGD sequence to circularize, thereby constraining several torsion angles of the C-alpha backbone. We made the 4C mutant to both the N-terminus of PlyCB (Fig. 2c) and the N-terminus of the 8-deletion mutant (Fig. 2d). Thus, we made a total of five unique RGD mutants.

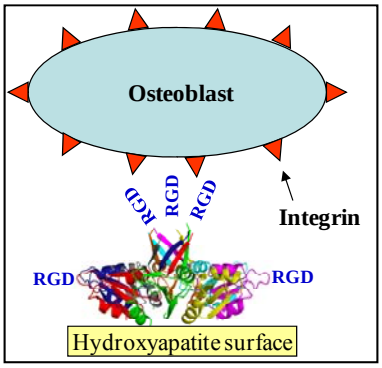

Fig. 1. Crystal structure of PlyCB octamer and optimal regions for insertion of RGD sequence motif.

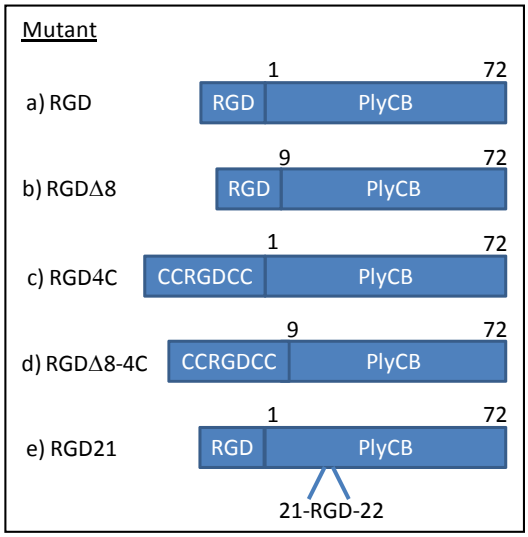

Fig. 2. Cartoon depiction of the five RGD mutants as described in the text.

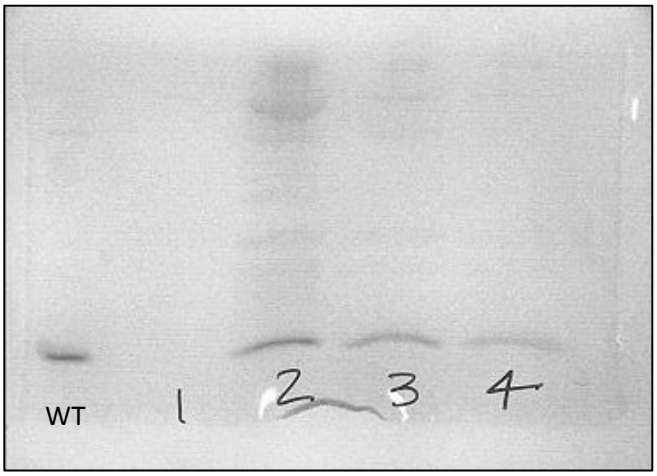

Fig. 3. Expression of RGD mutants. WT, PlyCB wild-type (8 kDa); 1, RGDΔ8-4C; 2, RGDΔ8; 3, RGD; 4, RGD-4C. Note, RGD21 not shown.

Of the five RGD mutants, three of them expressed as soluble proteins that migrated on an SDS-PAGE at 8 kDa, consistent with wild-type (WT) PlyCB (Fig. 3). Unfortunately, RGDΔ8-4C and RGD21 (data not shown on gel in Fig. 3) misfolded and formed insoluble inclusion bodies. Attempts to refold by protein via 8M urea and column chromatography in decreasing amounts of urea were unsuccessful (data not shown). Nonetheless, we expected some of the mutants to misfold, which is the reason we made five of them to evaluate. On the other hand, RGD, RGDΔ8, and RGD-4C all formed

soluble proteins of ~8 kDa. These three were purified to homogeneity and subjected to further biochemical and biophysical tests.

Task 3. Compare properties of PlyCB-RGD mutants to wild-type PlyCB. (months 6-10)

Our RGD, RGDΔ8, and RGD-4C mutants were compared to WT PlyCB. As stated above, all expressed as soluble proteins and migrated as an 8 kDa monomer on SDS-PAGE, identical to WT. All were subjected to analytical gel filtration to confirm formation of the octameric ring, which is a hallmark of PlyCB. As an example, Fig. 4 shows PlyCB-RGD (in red) migrating between the 44 kDa and 158 kDa standards (in blue) on a Superose 12 gel filtration column. This corresponds identically to the migration of WT PlyCB, which forms a 64 kDa octamer. All three mutants likewise were shown to form the octamer by gel filtration. Furthermore, all showed similar spectra on circular dichroism and none of the mutants or WT PlyCB displayed any thermal denaturation up to 60C (data not shown). Finally, similar to WT PlyCB none of the mutants has His-tags or other tags for purification. Rather, we took advantage of the strong binding properties of this protein to hydroxyapaptite and employed a ceramic hydroxyapaptite column for purification. All mutants were required >500 mM phosphate buffer for elution from this column. Thus, we conclude that incorporation of the RGD sequence motif to all three mutants did not alter the biochemical, binding, or structural properties of the PlyCB octamer.

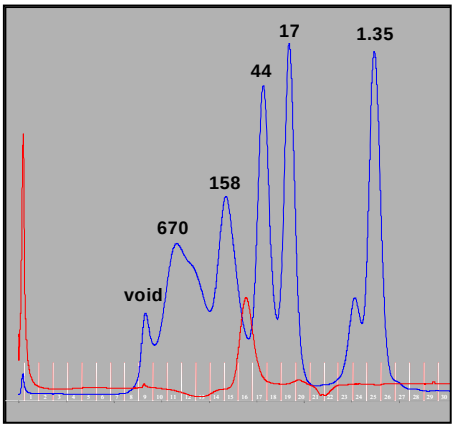

Fig. 4. Gel filtration on Superose 12 column of PlyCB-RGD (red). Bio-Rad gel filtration standards are shown on the blue chromatogram.

Aim 2. Determine binding properties of PlyCB-RGD mutants to hydroxyapatite (HA) and tricalcium phosphate (TCP).

Task 1. Show direct binding of PlyCB-RGD mutants to HA and TCP. (months 10-12)

There is a bit of confusion about HA and TCP in the literature that should be cleared up here. Several papers refer to each as the mineral component of bone and the coating most commonly applied to orthopedic implanted devices. HA is hydroxyapatite. It's formula is $Ca_5(PO_4)_3(OH)$, but is sometimes represented as $Ca_{10}(PO_4)_6(OH)_2$. TCP is tri-calcium phosphate, which has the formula $Ca_3(PO_4)_2$, but for medical applications, it is always in the hydroxylated, apatite form (i.e. $Ca_5(PO_4)_3(OH)$). Thus, for our purposes, HA and TCP are synonymous. Additionally, these compounds are used in a crystalline form, which is often referred to as "ceramic". Thus, from this point forward, we will refer to it as either HA, or ceramic HA, abbreviated CHA.

We chemically crosslinked WT PlyCB, PlyCB-RGD, and PlyCB-RGD-4C to Alexa-Fluor 525, a commercially available fluorophore. Each of the three fluorescently labeled proteins was then

mixed with 10 mg CHA in various buffers, ionic concentrations, pH, temperatures, and proteases. After a 30 min incubation under the various conditions, the mixture was centrifuged and the CHA pellet was separated from the aqueous supernatant. Each was assayed for total fluorescence on a 96-well fluorometer as shown in Figs. 5-9.

In all cases, PlyCB, PlyCB-RGD, and PlyCB-RGD-4C completely bound CHA in standard conditions. No fluorescence was detected in the supernatant. In non-standard conditions, the mutants displayed very robust binding properties comparable to WT PlyCB. Increasing ionic strength, up to 1M NaCl, had no negative consequence on binding to CHA (Fig. 5). Likewise, binding was not affected over a pH range of 4 to 9, and only showed diminished binding at pHs >10, which are not physiologically relevant (Fig. 6). The PlyCB mutants were also found to be very thermostable, able to maintain full binding to CHT at 60°C and had 50% binding at 70°C (Fig. 7). Finally, incubation with 10 µg/ml trypsin (Fig. 8) or chymotrypsin (Fig. 9) for up to 5 hours did not affect CHT binding of the mutants. This is an extremely important finding as proteases (i.e. matrix metalloproteases) are often associated with wound healing and may be present near implanted medical devices.

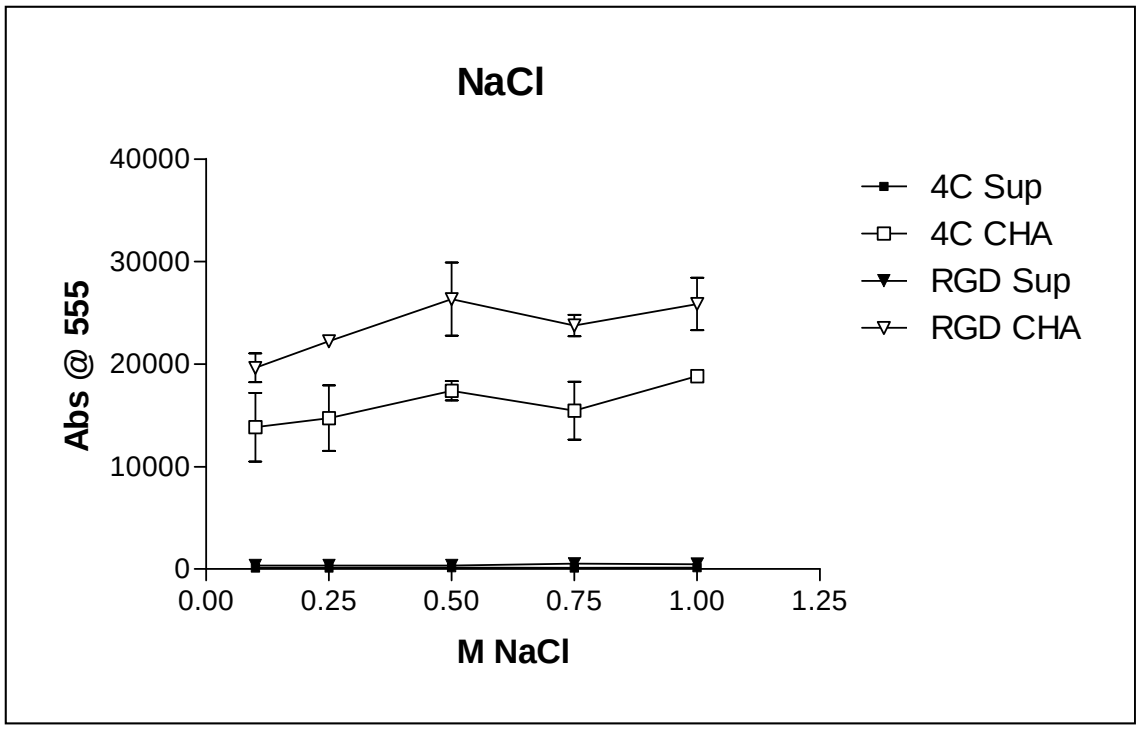

Fig. 5. Binding of PlyCB mutants to CHA is not affected by up to 1M NaCl.

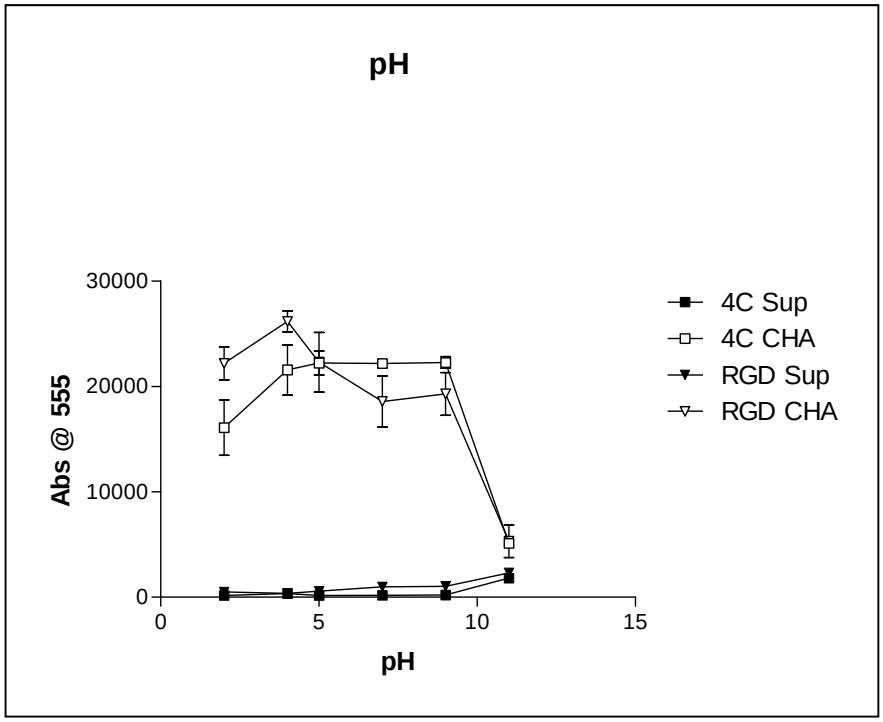

Fig. 6. Binding to CHA is stable between pH 4 and 9. Binding is only diminished at pHs >10.

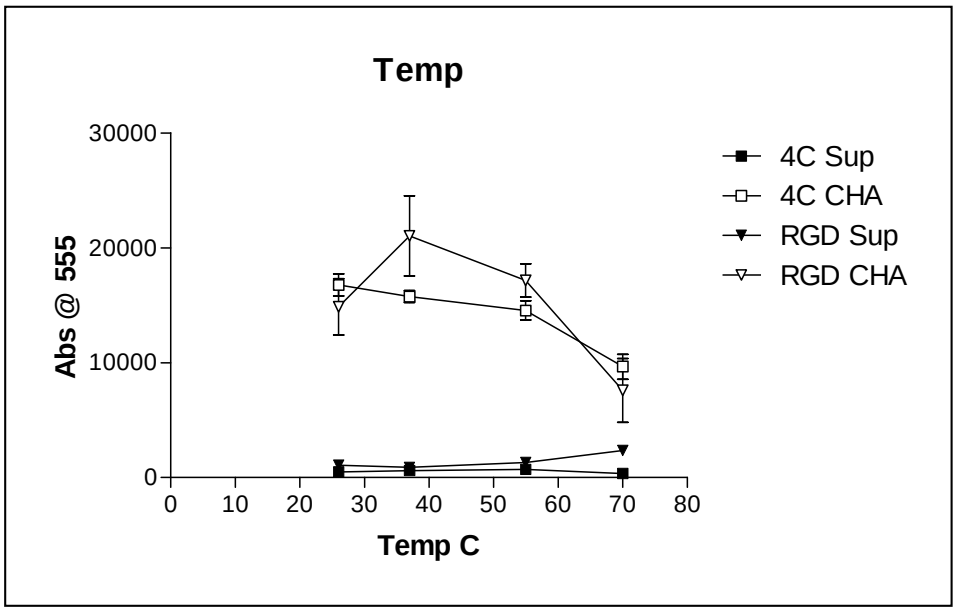

Fig. 7. Binding to CHA is stable between 25°C and 60°C for 30 min. At 70°C, ~50% of the PlyCB mutants remain bound.

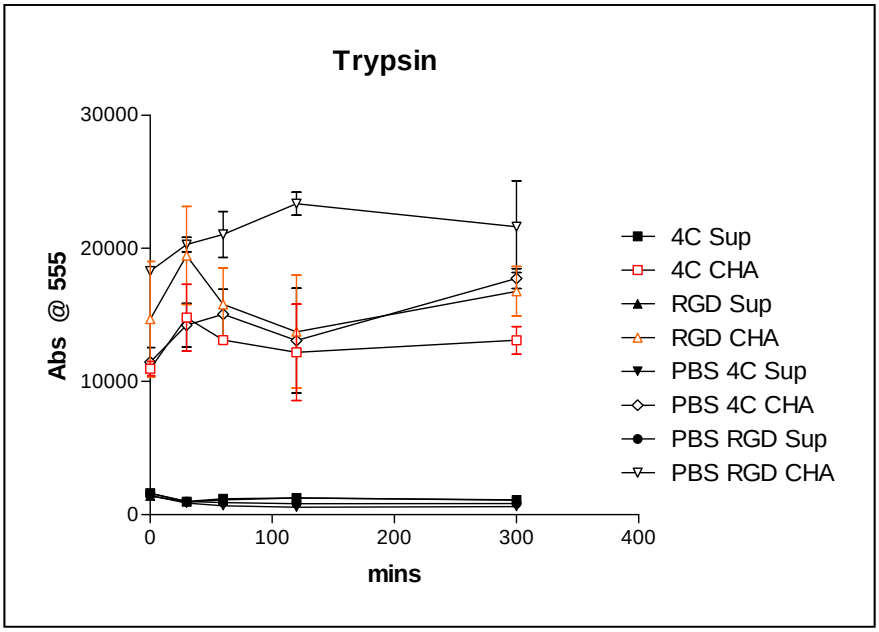

Fig. 8. Incubation with 10 µg/ml trypsin for up to 5 hours did not diminish binding of mutant PlyCB to CHT.

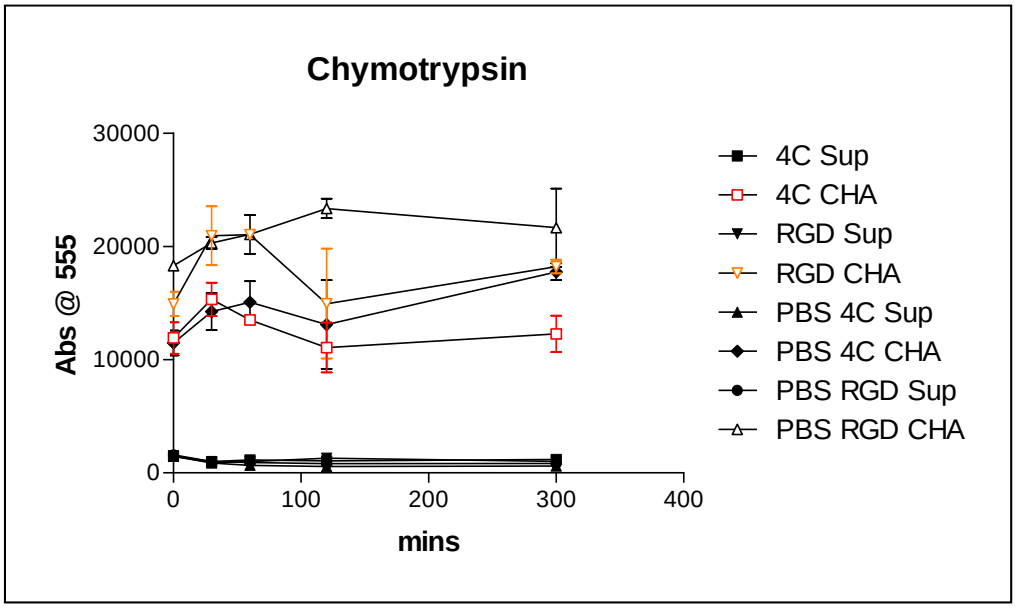

Fig. 9. Incubation with 10 µg/ml chymotrypsin for up to 5 hours did not diminish binding of mutant PlyCB to CHT.

Task 2. Determine binding constants for all PlyCB-RGD mutants to HA and TCP. (months 12-15)

Due to the solid state surface of HA, we were unable to perform Biacore-based surface plasmon resonance analysis. Therefore, in order to determine binding affinity of PlyCB to HA, we calculated apparent Kd's by fluorescent spectroscopy using phosphate titration curves. Breifly, PlyCB-RGD constructs were chemically crosslinked to the fluorophore AlexaFluor 488 and re-purified. The labeled protein was exposed to HA, followed by increasing concentrations of phosphate. At discrete phosphate concentrations, the supernatant was assayed for fluorescence to detect released PlyCB. A sample dataset is shown below in Fig 10. All constructs as well as WT PlyCB displayed similar tight affinity for HA with a Kd apparent ~10 nM.

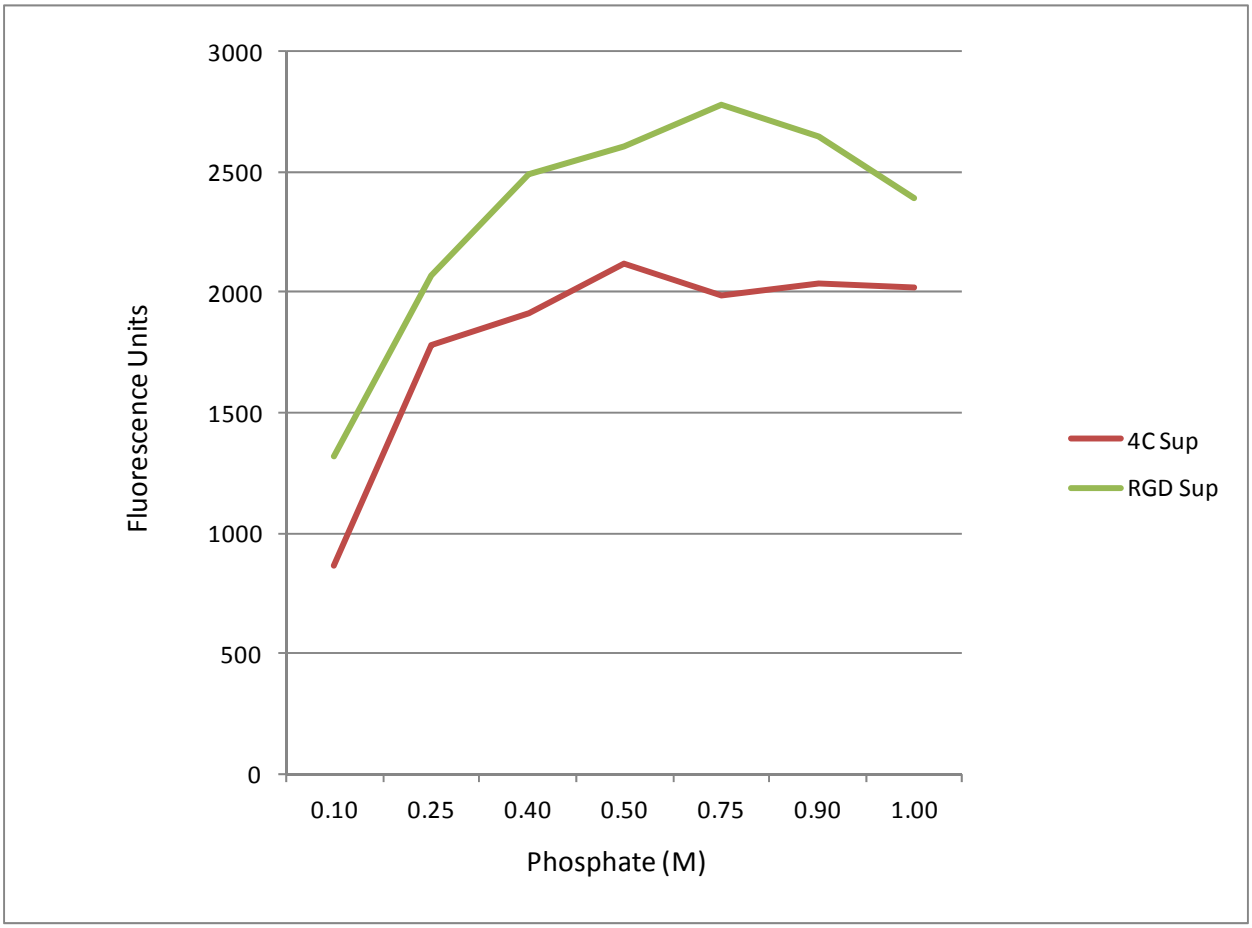

Fig. 10. AlexaFluor 488 labeled PlyCB-RGD constructs are released from HA with increasing phosphate concentration.

Aim 3. Show direct binding of PlyCB-RGD mutants to osteoblasts.

Task 1. Measure binding of PlyCB and PlyCB-RGD mutants to $\alpha_v\beta_3$ -specific integrins by enzyme-linked immunosorbant assay (elisa). (months 12-15)

PlyCB and the PlyCB-RGD mutants were spotted on a PVDF membrane. The membrane was blocked with 3% BSA, and 5 ug of $\alpha_v\beta_3$ was added. After a second wash step, FITC-labeled anti-$\alpha_v\beta_3$ antibodies were added to the wash solution. The PVDF membrane was dried and viewed by on a fluorescent dissecting microscope (Fig. 11). As can be seen, only constructs containing RGD cross reacted with the antibodies.

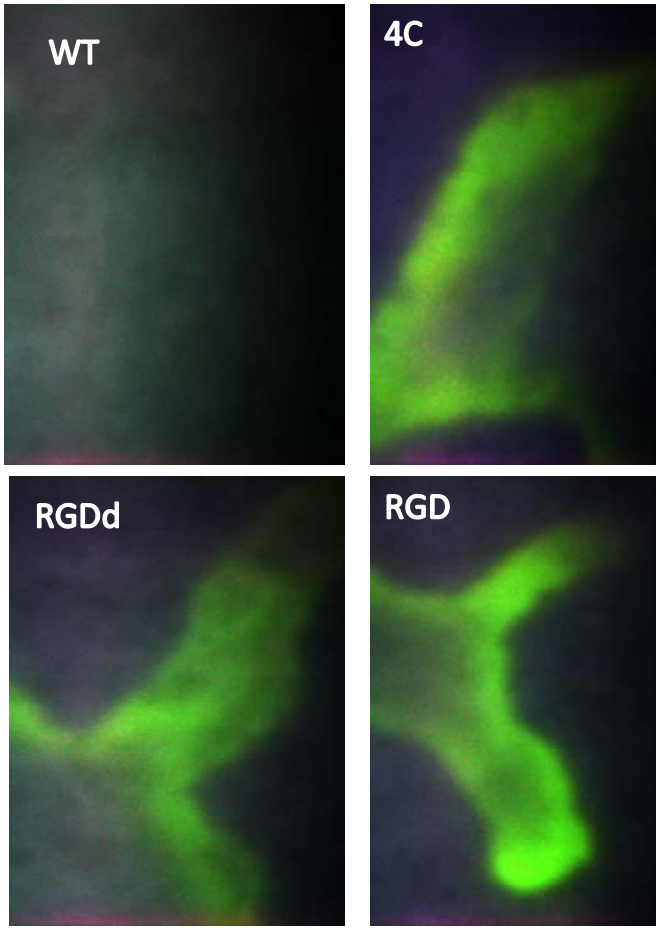

Fig. 11. Spot blot showing specific labeling of PlyC-RGD mutants, but not WT PlyC, with $\alpha_v\beta_3$.

Task 2. Use the AlexaFluor-labeled PlyCB and PlyCB-RGD mutants made in Aim 2.1, show specific and direct binding of the RGD mutants to cultured live osteoblasts. (months 12-15)

Cultured osteoblasts were exposed to AlexaFluor labeled PlyC or PlyC-RGD mutants (Fig. 12). Only the RGD mutants displayed binding to osteoblasts. Note, the nucleus of the ostoblasts is stained blue (DAPI) and AlexaFluor PlyCB constructs is shown in red.

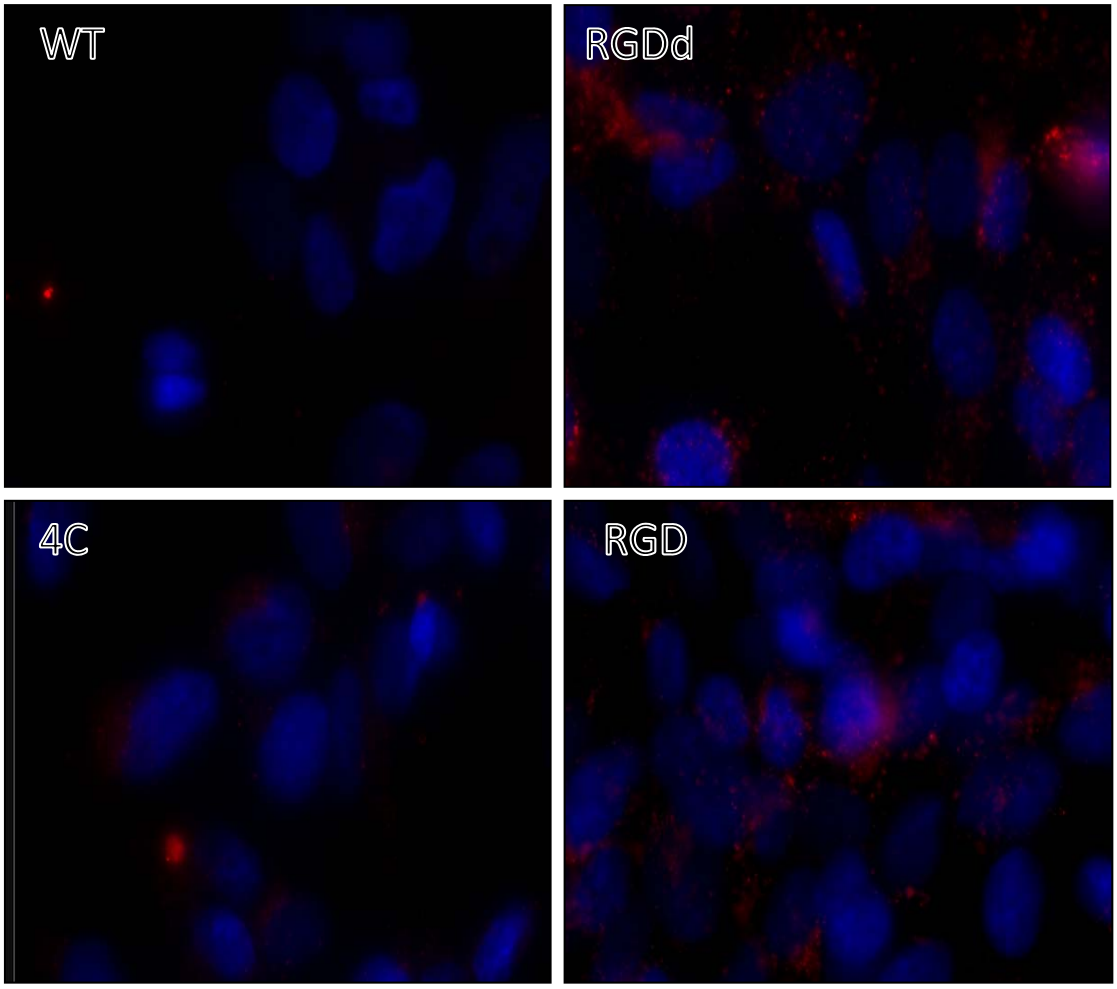

Fig. 12. Specific labeling of osteoblasts by PlyCB-RGD constructs, but not WT PlyCB. Blue: DAPI; Red: PlyCB/AlexaFluor525.

Task 3. Capture assay demonstrating osteoblast binding to PlyCB-coated titanium. (months 15-18)

HA-coated titanium discs were dipped in PlyCB or PlyCB-RGD constructs, allowed to dry, and placed in a 6 well tissue culture flask containing osteoblasts. After 4 hours, the titanium/culture medium interface was visualized by microscopy. As can be seen in Fig. 13, osteoblasts were readily attracted to PlyC-RGD and PlyCB-RGD4C, but not WT PlyC or PlyC-RGDdelta8. This proves that PlyC-RGD not only binds HA, but the RGD is displayed and attracts $\alpha_v\beta_3$ bearing osteoblasts.

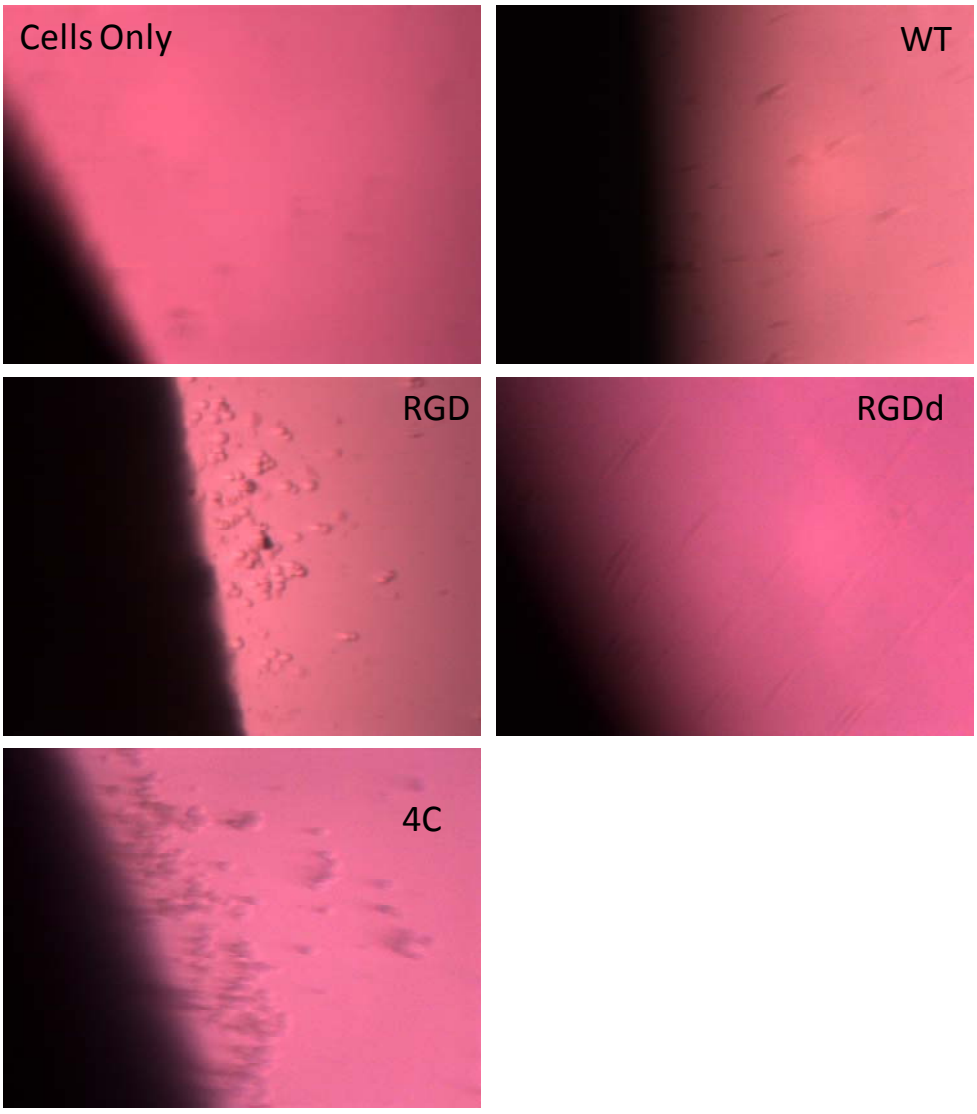

Fig. 13. Attraction of osteoblasts to HA-coated titanium discs bearing PlyCB-RGD and PlyCB-RGD4C, but not WT PlyCB or PlyCB-RGDdelta8. Note, the titanium is the black object on the left side of the field.

KEY RESEARCH ACCOMPLISHMENTS:

- Successfully made 3 soluble mutants to PlyCB, including those that display both linear and cyclic RGD epitopes.
- Demonstrated that insertion of RGD epitopes did not alter biochemical, binding, or structural properties of the protein.
- Demonstrated robust binding properties of the mutants to CHT, including broad temperature and pH ranges and tolerance to high ionic strength and proteases.
- Demonstrated high affinity (nanomolar) binding between PlyCB and HA.
- Showed direct binding of PlyCB-RGD mutants to $\alpha_v\beta_3$ integrins.
- Showed direct binding of PlyCB-RGD mutants to osteoblasts bearing $\alpha_v\beta_3$ integrins.
- Showed enhanced attraction and binding of osteoblasts to HA-coated titanium discs exposed to PlyCB-RGD.

REPORTABLE OUTCOMES:

Some aspects of our preliminary data and/or overall strategy have been presented at the following meetings/symposia during the past year:

- Georgia Institute of Technology, Atlanta, GA. Seminar speaker.
- Catholic University, Washington, D.C. Seminar speaker.
- Rockefeller University, New York, NY. Seminar speaker.

Based on the solid findings generated from this proposal, the PI submitted another proposal to DARPA in order to extend this line of work. The new proposal, "Engineering the biotic-abiotic interface of orthopedic implants" expands the concept of using PlyCB not only to display RGD sequences to attract osteoblasts, but building off the HA-PlyCB scaffold to display bone morphogenic peptides, angiogenesis peptides, and nerve growth peptides in order to generate new tissues following a traumatic battlefield injury. The proposal was in response to the Young Faculty Award (DARPA-RA-12-12) and was submitted January, 2012.

CONCLUSION:

Our results have met and exceeded our expectations. We have cloned, purified, and characterized several mutants of PlyCB that display robust stability and binding properties to CHT. Moreover, we have shown specific binding of our PlyCB-RGD mutant to $\alpha_v\beta_3$ integrins, osteoblasts, and concurrent binding to HA-coated titanium and osteoblasts. Thus, we have successfully engineered the biotic/abiotic orthopedic surface to promote osseointegration. Now that the data has been fully collected during the contract period, we intent to write up our results for peer reviewed publication. Once a manuscript is accepted, we will forward a copy to the CDMRP Scientific Officer.

REFERENCES:

Axelrad, T.W., Kakar, S., & Einhorn, T.A. (2007) New technologies for the enhancement of skeletal repair. *Injury* 38S1:S49-S62.

Carson, J.S. & Bostrom, M.P.G. (2007) Synthetic bone scaffolds and fracture repair. *Injury* 38S1:S33-S37.

Nelson, D., Schuch, R., Chahales, P. Zhu, S., & Fischetti, V.A. (2006) PlyC: A Multimeric Bacteriophage Lysin. *Proc. Natl. Acad. Sci. U.S.A*. 103:10765-10770.

Schuler, M., Trentin, D., Textor, M., & Tosatti, S.G.P. (2006) Biomedical interfaces: titanium surface technology for implants and cell carriers. *Nanomedicine* 1(4):449-463.

Tsiridis, E., Upadhyay, N., & Giannoudis, P. (2007) Molecular aspects of fracture healing: Which are the important molecules? *Injury* 38S1:S11-S25.

APPENDICES:

None.

SUPPORTING DATA:

Figures and figure legends are contained within the body of the text above.